Effect of mid-term drought on *Quercus pubescens* BVOCs emissions seasonality and their dependence to light and/or temperature

Amélie Saunier[1], Elena Ormeño[1], Christophe Boissard[2], Henri Wortham[3], Brice Temime-Roussel[3], Caroline Lecareux[1], Alexandre Armengaud[4], Catherine Fernandez[1].

[1]Aix Marseille Univ, Univ Avignon, CNRS, IRD, IMBE, Marseille, France.

[2]Laboratoire des Sciences du Climat et de l'Environnement, LSCE/IPSL, CEA-CNRS-UVSQ, Université Paris-Saclay, F-91191 Gif-sur-Yvette, France.

[3]Aix Marseille Univ, CNRS, LCE, Laboratoire de Chimie de l'Environnement, Marseille, France

[4] Air PACA, 146 rue Paradis, Bâtiment Le Noilly Paradis, 13294 Marseille, Cedex 06.

Correspondence to: Amélie Saunier (amelie.saunier@imbe.fr)

Key words: BVOCS, natural and amplified drought, season, light and temperature

Abstract. Biogenic volatile organic compounds (BVOCs) emitted by plants represent a large source of carbon compounds released into the atmosphere where they account for precursors of tropospheric ozone and secondary organic aerosols. Being directly involved in air pollution and indirectly in climate change, understanding what factors drive BVOCs is a prerequisite for modelling their emissions and predict air pollution. The main algorithms currently used to model BVOCs emissions are mainly light and/or temperature dependent. Additional factors such as seasonality and drought also influence isoprene emissions, especially in the Mediterranean region which is characterized by a rather long drought period in summer. These factors are increasingly included in models but only for the principal studied BVOC, namely isoprene but there are still some discrepancies in estimations of emissions. In this study, the main BVOCs emitted by *Quercus pubescens*: isoprene, methanol, acetone, acetaldehyde, formaldehyde, MACR MVK and ISOPOOH (these 3 last compounds detected under the same ion), were monitored with a PTR-ToF-MS over an entire seasonal cycle, under both *in situ* natural and amplified drought which is expected with climate change. Amplified drought impacted all studied BVOCs by reducing emissions in spring and summer while increasing emissions in autumn. All six BVOCs monitored showed daytime light and temperature dependencies while three BVOCs (methanol, acetone and formaldehyde) also showed emissions during the night despite the absence of light under constant temperature. Moreover, methanol and acetaldehyde burst in the early morning and formaldehyde deposition/uptake were also punctually observed which were not assessed by the classical temperature and light models.

1 Introduction

Plants contribute to global emissions of volatile organic compounds (VOCs) with an estimated emission rate of 10^{15} gC yr^{-1} (Guenther *et al.* 1995; Harrison *et al.* 2013). The large variety of compounds released by plants represents, at the global scale, 2-3% of the total carbon released in the atmosphere (Kesselmeier & Staudt 1999). Under strong photochemical conditions, BVOCs, together with NO_x, can significantly contribute to tropospheric ozone concentration (Xie *et al.* 2008; Papiez *et al.* 2009). In addition to its greenhouse effect, O_3 has strong effects on plant metabolism (Reig-Armiñana *et al.* 2004; Beauchamp *et al.* 2005) as well as on human health (Lippmann 1989). BVOCs are also rapidly oxidized by OH radical and NO_3 (Hallquist *et al.* 2009; Liu *et al.* 2012), which account for an important fraction of the total mass of secondary organic aerosols (SOA, Jimenez *et al.* 2009). Methanol and acetone are, after isoprene, the principal BVOCs released to the atmosphere. Isoprene emissions represent between 400-600 TgC yr^{-1} at the global scale (Arneth *et al.* 2008) whereas methanol emissions vary between 75 and 280 TgC yr^{-1} (Singh *et al.* 2000; Heikes *et al.* 2002, respectively) and acetone emissions represent only 33 TgC yr^{-1} (Jacob *et al.* 2002). Other compounds such as acetaldehyde, methacrolein (MACR), methyl vinyl ketone (MVK), isoprene hydroxy hydroperoxides (ISOPOOH) and formaldehyde, whose biogenic origin has been poorly investigated, are better known to be anthropogenic and/or secondary VOCs issued from atmospheric oxidations (Hallquist *et al.* 2009). However, acetaldehyde is also a by-product of plant metabolism and its emissions represent 23 Tg yr^{-1} at the global scale (Millet *et al.* 2010). Formaldehyde, MACR, MVK and ISOPOOH are released by plants through oxidations of methanol and isoprene, respectively, within leaves but they can have other leaf precursors (Oikawa & Lerdau 2013). Thus, it is thereby important to model all this panel of BVOCs emissions with the aim of predicting their effect on secondary atmospheric chemistry.

Current models allow to predict BVOCs emissions according to the type of vegetation, biomass density, leaf age, specific emission factor for many vegetal species, as well as the impact of some environmental factors. Models, such as the MEGAN (Guenther *et al.* 2006; Guenther *et al.* 2012) or CHIMERE (Menut *et al.* 2014) model, include at least two main algorithms that allow to model light and temperature emissions dependence (called *L+T* algorithm afterwards) and a temperature dependent algorithm (called *T* algorithm afterwards), both described in Guenther *et al.* (1995). The L+T algorithm is typically used for BVOCs emissions whose synthesis rapidly relies on photosynthesis, and hence include *de novo* emissions. The T algorithm is used for BVOCs emissions that do not directly rely on BVOCs synthesis when, for example, they originate from permanent large storage pools (Ormeno *et al.* 2011). The dependence to light and/or temperature is well documented for isoprenoids (Owen *et al.* 2002; Rinne *et al.* 2002; Dindorf *et al.* 2006) but there is still a lack of knowledge about highly volatile BVOCs (e.g. methanol, acetone, acetaldehyde). However, many of these compounds are very reactive in the atmosphere (Hallquist *et al.* 2009) and, could be emitted in large quantities to the atmosphere at global scale. The characterization of their emissions and sensitivity to light and/or temperature is, thus, necessary in order to obtain reliable predictions of atmospheric processes in order not to miss this important part of the atmospheric reactivity.

Other factors than light and temperature can drive BVOCs emissions such as water stress. Most studies dealing with BVOCs response to water stress have, however, focused on terpene-like compounds and have been carried out after weeks of watering restriction or removal under controlled conditions (for a review, see studies cited in Peñuelas and Staudt 2010). These studies reveal that there are still some misunderstandings at the level of emission mechanisms since some works showed increases (Funk *et al.* 2004; Monson *et al.* 2007) or decreases of isoprene emissions (Brüggemann & Schnitzler 2002; Fortunati *et al.* 2008) and there is a lack of knowledge

on the impact of water stress on highly BVOCs emissions. Moreover, the sensitivity of isoprene and highly volatile BVOCs emissions to recurrent water stress (few years) under *in situ* conditions is clearly missing. Likewise, the capacity of current *L+T* and *T* algorithms to predict emission shifts under different drought scenarios in the context of climate change needs to be addressed for isoprene and highly volatile compounds. This is of especial interest for the Mediterranean area where the most severe climatic scenario of the IPCC predicts an intensification of summer drought consisting on a rain reduction that can locally reach 30%, an extension of the drought period as well as a temperature rise of 3.4°C, (Giorgi & Lionello 2008; IPCC 2013; Polade *et al.* 2014) for 2100.

In the present investigation, we aimed (i) to study the standard emission factors of each studied BVOC released by *Q. pubescens,* including isoprene and highly volatile compounds that originate from plant metabolism under water stress (ii) to test the performance of the L+T and T algorithms to predict isoprene and highly volatile BVOCs emissions over the seasonal cycle and under two recurrent water stress treatments. *Q. pubescens* was chosen as vegetal model because this species is highly resistant to drought and well widespread in the Northern Mediterranean area occupying 2 million ha (Quézel & Médail 2003). It also represents the major source of isoprene emissions in the Mediterranean area and the second one at the European scale (Keenan *et al.* 2009).

2 Material and methods

2.1 Experimental site

Our study was performed at the O_3HP site (Oak Observatory at OHP, Observatoire de Haute Provence), located 60 km North of Marseille, France (5°42'44" E, 43°55'54" N), at an elevation of 650m above the sea level. The O_3HP (955m^2), free from direct human disturbance for 70 years, consists of a homogeneous forest mainly composed of *Q. pubescens* (≈ 90 % of the biomass and ≈ 75 % of the trees) with a mean diameter of 1.3 m. The remaining 10 % of the biomass is mainly represented by *Acer monspessulanum* trees, a very low isoprene-emitter species (Genard-Zielinski *et al.* 2015). The O_3HP site was created in 2009 in order to study the impact of climate change on a *Q. pubescens* forest. Using a rainfall exclusion device (an automated monitored roof deployed during rain events) set up over part of the O_3HP canopy, it was possible to reduce natural rain by 30% and to extend the drought period in an attempt to mimic the current climatic model projections for 2100 (Giorgi & Lionello 2008; IPCC 2013; Polade et al. 2014). Two plots were considered in the site; a plot receiving natural precipitation where trees grew under natural drought (300m² surface, used as control plot) and a second plot submitted to amplified drought (232m² surface, used as amplified drought plot). Rain exclusion on this latter plot started on April 2012 and was continuously applied every year, principally, during the growth period. Ombrothermic diagrams indicated that the drought period was extended for 2 months in 2012, 4 months in 2013 and 3 months in 2014 for amplified drought relative to natural drought (Fig 1). Data on cumulative precipitation showed that 35% of rain was excluded in 2012 (from 29 April from to 27 October), 33.5% in 2013 (from 7 July from to 29 December), 35.5% in 2014 (from 8 April to 8 December). This experimental set up involved a recurrent drought in the amplified drought plot. Sampling was performed at the branch-scale at the top of the canopy during three campaigns from October 2013 to July 2014, covering an entire seasonal cycle: in autumn (14 to 28 October 2013, 2nd year of amplified drought), in spring (12 to 19 May 2014, 3rd year of amplified drought) and in summer (13 to 25 July 2014, 3rd year of amplified drought). Spring, summer and autumn

campaigns corresponded to the end of leaf growth, leaf maturation and the beginning of the leaf senescence, respectively. The same five trees per plot were selected and investigated throughout the study.

2.2 Branch scale-sampling methods

Two identical dynamic branch enclosures were used for sampling gas exchange (in terms of CO_2, H_2O and BVOCs) as fully described in Genard-Zielinski *et al.* (2015) with some modifications. Branches were enclosed in a ≈ 30L PTFE (polytetrafluoroethylene) frame closed by a 50µm thick PTFE film. One tree from natural and one tree from amplified drought plot were analysed concomitantly during 1 or 2 days. Inlet air was introduced at 9L.min^{-1}, controlled by mass flow controllers (MFC, Bronkhorst), using an air generator made, inside, by PTFE (KNF N840.1.2FT.18®, Germany) allowing for air renewal inside the chamber every ~ 3min. Ozone was removed from inlet air by placing PTFE filters impregnated with sodium thiosulfate ($Na_2S_2O_3$) as described by Pollmann *et al.* (2005), so that oxidation of BVOCs due to ozone within the enclosed atmosphere is negligible. The excess of air humidity was removed using drierite. A PTFE fan ensured a rapid mixing of the chamber air and a slight positive pressure within the enclosure enabled the PTFE film to be held away from leaves to minimise biomass damage. Microclimate (temperature, relative humidity and photosynthetically active radiation or PAR) was continuously (every minute) monitored by a data logger (LI-COR 1400®; Lincoln, NE, USA) with a relative humidity and temperature probe placed inside the chamber (RHT probe, HMP60, Vaisala, Finland) and a quantum sensor (PAR, LI-COR, PAR-SA 190®, Lincoln, NE, USA) placed outside the chamber. The climatic conditions in terms of PAR and temperatures are summarized in Fig. S1 (in supplementary files) for each field campaigns. All air flow rates were controlled by mass flow controllers (MFC, Bronkhorst) and all tubing lines were made of PTFE. Chambers were installed the day before measurements and flushed overnight. Enclosed branches contained 8 to 12 leaves corresponding to a range of 1.4 to 3.6g of dry matter and 110 to 320cm² of leaf surface, respectively

2.3 Ecophysiological parameters

Exchanges of CO_2 and H_2O from the enclosed branches were continuously (every min) measured using infrared gas analysers (IRGA 840A®, LI-COR) concomitantly with BVOCs emission measurements (cf. 2.4). Gas exchange values were averaged by taking into account all the data measured between 12h and 15h (local time). Net photosynthesis (*Pn*, µmolCO_2 m^{-2} s^{-1}) and stomatal conductance to water (*Gw*, mmolH_2O m^{-2} s^{-1}) were calculated using equations described by Von Caemmerer and Farquhar (1981) as used in Genard-Zielinski *et al.* (2015) (for more details, see Appendix A, equations A1 to A4). Leaves from enclosed branches were directly collected after gas exchange sampling to accurately measure leaf surface with a leaf area meter. Gas exchange were hence expressed in a leaf surface basis. After that, leaves were freeze-dried to assess their dry mass.

2.4 BVOCs analysis

A PTR-ToF-MS 8000 instrument (Ionicon Analytik GmbH, Innsbruck, Austria) was used for online measurements of BVOCs emitted by the enclosed branches. A multi-position common outlet flow path selector valve system (Vici) and a vacuum pump were used to sequentially select air samples from: amplified drought, inlet air, natural drought, ambient air and catalyser. Each sample was analysed every hour, with 15min of

analysis. Mass spectra in the range 0-500amu were recorded at 1min integration time. The reaction chamber pressure was fixed at 2.1mbar, the drift tube voltage at 550V and the drift tube temperature at 313 K corresponding to an electric field strength applied to the drift tube (E) to a buffer gas density (N) ratio of 125Td (1Td = 10^{-17} V cm^2). A calibration gas standard (TO-14A Aromatic Mix, Restek Corporation, Bellefonte, USA, 100 ± 10ppb in Nitrogen) was used to experimentally determine the ion relative transmission efficiency. BVOCs targeted in this study and their corresponding ions include formaldehyde (m/z 31.018), methanol (m/z 33.033), acetaldehyde (m/z 45.03), acetone (m/z 59.05), isoprene (m/z 41.038, 69.069) and MACR+MVK+ISOPOOH (m/z 71.049, these three compounds were detected with the same ion with PTR-MS). The signal corresponding to protonated VOCs was converted into mixing ratios by using the proton transfer rate constants k given by Cappellin *et al.* (2012). Formaldehyde concentrations were calculated according to the method described by Vlasenko *et al.* (2010) to account for its humidity dependent sensitivity.

BVOCs emissions rates (ER) were calculated by considering the BVOCs concentrations in the inlet and outlet air as follows (equation 1):

$$ER = \frac{Q_0 * (C_{out} - C_{in})}{B} \quad (1)$$

where *ER* was expressed in µgC g_{DM}^{-1} h^{-1}, Q_0 was the flow rate of the air introduced into the chamber (L h^{-1}), C_{out} and C_{in} were the concentrations in the inflowing and outflowing air (µgC L^{-1}), respectively, and B was the total dry biomass matter (g_{DM}). Daily cycles were made by averaging measured emissions of all trees every hour.

2.5 Emission algorithms

The light and/or temperature dependence of *Q. pubescens* BVOCs (isoprene and highly volatile compounds) under natural and amplified drought was tested using both the *L+T* and *T* algorithms. Emission rates calculated according to these algorithms (called afterwards ER_{L+T} and ER_T, respectively) were calculated using the equation described in Guenther *et al.* (1995) (for more details, see Appendix B, equations B1 to B5). The empirical coefficient β (used in the *T* algorithm) was determined for each compound according to the season and the treatment through the slope of correlation between the natural logarithm of emissions rates (measured emissions, µgC g_{DM}^{-1} h^{-1}) and experimental temperature (K). Standardised emissions rates (*EF*, emissions rates at standard conditions of light and temperature, 1000µmol m^{-2} s^{-1} and 30°C), were used to calculate modelled emissions. *EF* were determined for each compound according to the season and the treatment and corresponded to the slope of the correlation between experimental emission rates and values of $C_l * C_t$ when using the *L+T* algorithm or C_T when using the *T* algorithm (see Appendix B for a full description of $C_l * C_t$ and C_T). All parameters used for the calculation of modelled emissions are presented in supplementary files (Table S1).

2.6 Data treatment

Data treatment was performed with the software STATGRAPHICS® centurion XV (Statpoint, Inc). After having checked the normality of the data set, two-way repeated measures ANOVA were performed to evaluate the variability of *Pn*, *Gw* and BVOCs emission rates according to the drought treatment and the season. Pearson's correlations between measured and modelled emissions were performed to evaluate the algorithm (*L+T* or *T*) that better predicted *Q. pubescens* emissions under the different drought conditions and over the

seasonal cycle. Afterwards, linear regressions tests and slope comparison tests (equal to 1, referred to "sl" afterwards) were also performed to evaluate the good fit of tested algorithms with BVOCs emissions rates.

3. Results and discussion

3.1 Ecophysiological parameters

The physiology of *Q. pubescens* was slightly impacted by amplified drought (Fig. 2), over the whole study, with a decrease of *Gw* under amplified drought compared to natural drought, by 44 % in spring ($P < 0.1$) and 55 % in summer ($P < 0.01$, Table 1). In autumn, there was no significant difference between both treatments. Pn was only reduced in summer by 36 % ($P < 0.1$) and there was no difference for the others season. Thus, the stomatal closure observed had a slight impact on carbon assimilation. Indeed, *Q. pubescens* has a high stem hydraulic efficiency (Nardini & Pitt 1999) which compensates the stomatal closure since it allows to use water more efficiently, thus, maintaining *Pn*. Moreover, it must be noted that an increase of Pn was observed in autumn and could likely be attributed to the autumnal rains. These results showed that the amplified drought artificially applied to *Q. pubescens* at O_3HP led to a moderate drought for this species, based on a moderate reduction of the physiological performances (Niinemets 2010).

3.2 Effect of drought on BVOCs emissions

The emissions of all BVOCs followed during this experimentation were reduced under amplified drought compared to natural drought, especially in spring and summer (Table 1) except for acetaldehyde emissions. Indeed, for this compound, there was no significant difference between both treatments probably due to a large variability of the data set. In autumn, for all BVOCs, there was no difference between both plots. The decrease of oxygenated BVOCs in spring and summer under amplified drought (e.g. methanol, MACR+MVK+ISOPOOH, formaldehyde, acetone) could be explained by the concomitant stomatal closure in spring and summer under amplified drought. Indeed, the emissions of these compounds are strongly bound to *Gw* (Niinemets *et al.* 2004). Isoprene emissions were also reduced in spring and summer during the third year of this experiment whereas an increase was observed in the first year (personal communication from A.C Génard-Zielinski) as well as what had been shown by Brüggemann and Schnitzler (2002) but this work was conducted with potted plants. The isoprene decrease observed in our experiment cannot be explained by the stomatal closure because this compound could also be emitted through the cuticle (Sharkey & Yeh 2001). It could rather be due to the decrease of *Pn* which reduced the carbon availability to produce isoprene. Moreover, carbon assimilated through *Pn* can be also invested into the synthesis of other defense compounds leading to a decrease of isoprene production and emission.

3.3 Effect of drought on light and/or temperature dependence through a seasonal cycle

All six BVOCs monitored showed daytime light and temperature dependencies (isoprene, degradation products of isoprene and acetaldehyde), while three BVOCs (methanol, acetone and formaldehyde) also showed emissions during the night despite the absence of light under constant temperature.

Regarding the light and temperature dependencies, the daily cycle of isoprene emissions (Fig. 3) showed that this compound responds strongly to light and temperature as already known (Guenther *et al.* 1993) and that this response was not impacted by amplified drought. Isoprene can protect thylakoids from oxidative damage (Velikova *et al.* 2011) occurring mainly during the day which can explain this kind of dependence. Yet, our results showed the importance to take into account the effect of amplified drought on emission factors because the intensity of isoprene emissions between natural and amplified drought was very different independently of the season. The modelled emissions were very representative of measured emissions except in spring for natural drought when we obtained a slight underestimation of emissions (sl = 0.84, $P < 0.05$) maybe, because light and temperature, in spring, were not the only parameters driving isoprene emissions. At this season, plants likely needed to produce more isoprene to protect the establishment of photosystems in the new leaves.

MACR+MVK+ISOPOOH emissions, as isoprene, seemed to respond better to light and temperature than to only temperature (Fig. S2 in supplementary files) since correlations between measured emissions and ER_{L+T} were always better than correlations with ER_T. Since MACR+MVK+ISOPOOH are oxidation products of isoprene (Oikawa & Lerdau 2013), it is not surprising that these compounds followed the same pattern than isoprene in terms of dependence to light and temperature. The estimations of ER_{L+T} were quite good except in spring under natural drought where a slight underestimation was observed (sl = 0.87, $P < 0.05$).

The dependence of acetaldehyde emissions to light and/or temperature is very contrasted; studies have shown that they are bound to both light and temperature (Jardine 2008; Fares *et al.* 2011) or to temperature only (Hayward *et al.* 2004). Our results suggested that acetaldehyde emissions were mainly bound to light and temperature (Fig. 4). Indeed, correlations between measured and ER_{L+T} were always better than with ER_T. However, some discrepancies were observed. Under natural drought, underestimations were observed in spring and summer (sl = 0.72, and sl = 0.57, $P < 0.05$, respectively) whereas in autumn, there was a good estimation (sl = 0.86, $P > 0.05$). Under amplified drought, underestimation was only observed in summer (sl = 0.80, $P < 0.05$). Daily cycles of acetaldehyde emissions presented also an emissions burst in the morning (at 7h, local time) in spring (under both treatments) and in summer (only under natural drought). Acetaldehyde can be produced due to an overflow of pyruvic acid during light-dark transitions. Cytosolic pyruvic acid levels rise rapidly and it can be converted into acetaldehyde by pyruvate decarboxylase (Fall 2003). This mechanism could explain the morning burst for this compound and the fact that no emissions during the night was observed

We observed emissions of methanol, acetone and formaldehyde during the night under no light and constant temperature (around 20°C, see supplementary files S1). Correlations between ER_{L+T} or ER_T and measured methanol emissions were very similar especially in spring and summer (Fig. 5). However, some observed phenomena suggested that methanol emissions was sustained by temperature alone at certain moment of the day. Indeed, the burst in the early morning (at 7h, local time), similar to acetaldehyde, was observed when stomata opened in spring and summer, independently of the drought treatment although it was clearer under natural than amplified drought. This burst can be explained by a strong release of this compound that has been accumulated in the intercellular air space and leaf liquid pools (due to the relative high polarity of methanol) at night when stomata are closed (Hüve *et al.* 2007). Moreover, for both drought treatments, methanol emissions during the night were observed at any seasons (especially autumn) which could be explained by nocturnal temperatures (roughly constant) that sufficed to maintain the biochemical processes involved in methanol formation. Methanol

emissions, which result from the demethylation of pectin during the leaf elongation, has already been described to be temperature dependent alone (Hayward *et al.* 2004; Folkers *et al.* 2008). However, our results suggest that methanol emissions respond strongly to light and temperature during the day. This kind of diurnal emissions cycle has already been described by Smiatek and Steinbrecher (2006). Our results about daily cycles of acetone emissions (Fig. S3 in supplementary files) showed that this compound responded better to light and temperature than only temperature since correlations were better with ER_{L+T}. Under natural drought, the modelled emissions were well representative of measured emissions in summer. By contrast, in spring and in autumn, slight underestimations were observed (sl = 0.88, $P < 0.05$ and sl = 0.69, $P < 0.05$, respectively). Under amplified drought, good estimations were observed in summer and autumn but in spring, there was an overestimation of modelled emissions (sl = 1.27, $P < 0.05$). Previous studies have shown that acetone rather depends on temperature alone (Fares *et al.* 2011) or to light and temperature (Jacob *et al.* 2002), indicating that its dependence to light and/or temperature remains unclear. During the day, acetone emissions were dependent to light and temperature and emissions still occurred during the night, especially in autumn. Alike methanol, nocturnal temperatures could allow to maintain acetone formation (Smiatek & Steinbrecher 2006). Acetone is a by-product of plant metabolism (Jacob *et al.* 2002) and its production can be enzymatic and non-enzymatic (Fall 2003) which can explain these observed differences through the day. We can suppose that acetone emissions observed during the day could come from the enzymatic activity and, on the contrary, during the night, they could come from the non-enzymatic production.

Formaldehyde emissions followed the same pattern than methanol and acetone emissions (Fig. S4 in supplementary files), especially in autumn. By considering only the daytime (correlation with $L+T$ modelled emissions), there were good estimations in summer and autumn and a slight underestimation was observed in spring (sl = 0.89, $P < 0.05$) for natural drought. Under amplified drought, correlations indicated that $L+T$ modelled emissions were well representative of measured emissions, but some negative emissions were observed in summer which suggested a deposition or an uptake of this compound by leaves as already highlighted by Seco *et al.* (2008). This phenomenon could have a role in stress tolerance, since formaldehyde can be catabolised (mainly through oxidations) within leaves leading to CO_2 formation (Oikawa & Lerdau 2013). Emissions during the night suggest that formaldehyde came from another source than oxidation within leaves since oxidations occur mainly during the day due to an excess of light in chloroplasts, principal place of reactive oxygen species production (Asada 2006). Thus, formaldehyde emissions observed during the night could result from, for example, the glyoxylate decarboxylation or the dissociation of 5,10-methylene-THF (Oikawa & Lerdau 2013).

4 Conclusion

After 3 years of amplified drought, all BVOCs emissions were reduced in spring and summer compared to natural drought whereas, in autumn, an increase was observed for some compounds. These results are in opposition with the results obtained after only one year of amplified drought (2012), especially for isoprene, where an increase was observed for this compound (personal communication from A.C. Génard-Zielinski). Amplified drought did not seem to shift the dependence to light and/or temperature which remained unchanged between treatments.

Moreover, two different dependence behaviours were found: (i) all six BVOCs monitored showed daytime light and temperature dependencies while (ii) only three BVOCs (methanol, acetone and formaldehyde) also showed that their emissions were maintained during the night with no light at rather constant nocturnal temperatures. Moreover, some phenomena, such as methanol and acetaldehyde emissions bursts in early morning or the formaldehyde deposition/uptake (formaldehyde), were not assessed by either *L+T* or *T* algorithm.

Appendix A: calculation of ecophysiological parameters

Net photosynthesis (Pn, µmolCO_2 m^{-2} s^{-1}) was calculated using equations described by Von Caemmerer and Farquhar (1981) as follows:

$$\mathrm{Pn} = \frac{F*(Cr-Cs)}{S} - CS*E \quad \text{(A1)}$$

Where *F* is the inlet air flow (mol s^{-1}), *Cs* and *Cr* are the sample and reference CO_2 molar fraction respectively (ppm), *S* is the leaf surface (m^2), *Cs*E* is the fraction of CO_2 diluted in water evapotranspiration and *E* (molH_2O m^{-2} s^{-1} then transformed in mmolH_2O m^{-2} s^{-1}, afterward) is the transpiration rate calculated as follow:

$$\mathrm{E} = \frac{F*(Ws-Wr)}{S*(1-Ws)} \quad \text{(A2)}$$

where *Ws* and *Wr* are the sample and the reference H_2O molar fraction respectively (molH_2O mol^{-1}).

Stomatal conductance to water (*Gw*, molH_2O m^{-2} s^{-1} then transformed in mmolH_2O m^{-2} s^{-1}) was calculated using the following equation:

$$\mathrm{Gw} = \frac{E*(1-\frac{Wl-Ws}{2})}{Wl-Ws} \quad \text{(A3)}$$

where *Wl* is the molar concentration of water vapour within the leaf (molH_2O mol^{-1}) calculated as follows:

$$Wl = \frac{Vpsat}{P} \quad \text{(A4)}$$

where Vpsat is the saturated vapour pressure (kPa) and P was the atmospheric pressure (kPa).

Appendix B: Modelled emissions calculation

The modelled emissions rates according to light and temperature (ER_{L+T}) or the temperature algorithm (ER_T) were calculated according to algorithms described in Guenther *et al.* (1995) as follows :

$$ER_{L+T} = EF_{L+T} * Cl * Ct \quad \text{(B1)}$$

where EF_{L+T} is the emission factor at 1000 µmol m^{-2} s^{-1} of photosynthetically active radiation (PAR) and 30°C of temperature (obtained with the slope of the correlation between experimental emissions and *Cl *Ct*), *Cl* and *Ct* correspond to light and temperature dependence factors respectively and were calculated with the following formulae:

$$Cl = \frac{\alpha C_{L1} L}{\sqrt{1+\alpha^2 L}} \quad \text{(B2)}$$

$$Ct = \frac{exp\,\frac{C_{T1}(T-T_S)}{RT_S T}}{1+exp\frac{C_{T2}(T-T_M)}{RT_S T}} \quad \text{(B3)}$$

where α = 0.0027, C_{L1} = 1.066, C_{T1} = 95000J mol^{-1}, C_{T2} =230000J mol^{-1}, T_M = 314K are empirically derived constants, L is the photosynthetically active radiation (PAR) flux (µmol m^{-2} s^{-1}), T is the leaf experimental temperature (K) and T_S is the leaf temperature at standard condition (303K).

Modelled emissions according to temperature alone that is ER_T, was calculated as follows:

$$ER_T = EF_T * C_T \quad \text{(B4)}$$

where EF_T is the emission factor at 30°C of temperature (obtained with the slope of the correlation between experimental emissions and C_T) and C_T is a temperature dependence factor calculated as follows:

$$C_T = \exp[\beta(T - T_S)] \quad \text{(B5)}$$

where β is an empirical coefficient (with a standard variation value of 0.09K^{-1} used in literature when not measured) determined, in this study, for each compound according to the season and the treatment through the slope of the correlation between the natural logarithm of measured emissions rates (ER, µgC g_{DM}^{-1} h^{-1}) and experimental temperature (expressed in K), T is the leaf experimental temperature (K) and T_S is the standard temperature (303K).

Author contribution

AS, EO and CF designed the research and the experimental design. AS, BTR, EO and CF conducted the research. AS, CB, BTR, and CL collected and analyzed the data. AS, EO, CB, HW, BTR, AA and CF wrote the manuscript

Competing interests

The authors declare that they have no conflict of interest.

Acknowledgment

This work was supported by the French National Agency for Research (ANR) through the SecPriMe² project (ANR-12-BSV7-0016-01); Europe (FEDER) and ADEME/PACA for PhD funding. We are grateful to FR3098 ECCOREV for the O_3HP facilities (https://o3hp.obs-hp.fr/index.php/fr/). We are very grateful to J.-P. Orts, I. Reiter. We also thank all members of the DFME team from IMBE and particularly: S. Greff, S. Dupouyet and A. Bousquet-Melou for their help during measurements and analysis. We thank also, the Université Paris Diderot-Paris7 for its support. The authors thank the MASSALYA instrumental platform (Aix Marseille Université, lce.univ-amu.fr) for the analysis and measurements used in this publication.

References

Arneth A., Monson R., Schurgers G., Niinemets Ü. & Palmer P. (2008). Why are estimates of global terrestrial isoprene emissions so similar (and why is this not so for monoterpenes)? *Atmospheric Chemistry and Physics*, 8, 4605-4620.

Asada K. (2006). Production and scavenging of reactive oxygen species in chloroplasts and their functions. *Plant physiology*, 141, 391-396.

Beauchamp J., Wisthaler A., Hansel A., Kleist E., Miebach M., NIINEMETS Ü., Schurr U. & WILDT J. (2005). Ozone induced emissions of biogenic VOC from tobacco: relationships between ozone uptake and emission of LOX products. *Plant, Cell & Environment*, 28, 1334-1343.

Brüggemann N. & Schnitzler J.P. (2002). Comparison of Isoprene Emission, Intercellular Isoprene Concentration and Photosynthetic Performance in Water-Limited Oak (Quercus pubescens Willd. and Quercus robur L.) Saplings. *Plant Biology*, 4, 456-463.

Cappellin L., Karl T., Probst M., Ismailova O., Winkler P.M., Soukoulis C., Aprea E., Märk T.D., Gasperi F. & Biasioli F. (2012). On quantitative determination of volatile organic compound concentrations using proton transfer reaction time-of-flight mass spectrometry. *Environmental science & technology*, 46, 2283-2290.

Dindorf T., Kuhn U., Ganzeveld L., Schebeske G., Ciccioli P., Holzke C., Köble R., Seufert G. & Kesselmeier J. (2006). Significant light and temperature dependent monoterpene emissions from European beech (Fagus sylvatica L.) and their potential impact on the European volatile organic compound budget. *Journal of Geophysical Research: Atmospheres*, 111.

Fall R. (2003). Abundant oxygenates in the atmosphere: a biochemical perspective. *Chemical reviews*, 103, 4941-4952.

Fares S., Gentner D.R., Park J.-H., Ormeno E., Karlik J. & Goldstein A.H. (2011). Biogenic emissions from Citrus species in California. *Atmospheric Environment*, 45, 4557-4568.

Folkers A., Hüve K., Ammann C., Dindorf T., Kesselmeier J., Kleist E., Kuhn U., Uerlings R. & Wildt J. (2008). Methanol emissions from deciduous tree species: dependence on temperature and light intensity. *Plant biology*, 10, 65-75.

Fortunati A., Barta C., Brilli F., Centritto M., Zimmer I., Schnitzler J.P. & Loreto F. (2008). Isoprene emission is not temperature-dependent during and after severe drought-stress: a physiological and biochemical analysis. *The Plant Journal*, 55, 687-697.

Funk J., Mak J. & Lerdau M. (2004). Stress-induced changes in carbon sources for isoprene production in Populus deltoides. *Plant, Cell & Environment*, 27, 747-755.

Genard-Zielinski A.-C., Boissard C., Fernandez C., Kalogridis C., Lathière J., Gros V., Bonnaire N. & Ormeño E. (2015). Variability of BVOC emissions from a Mediterranean mixed forest in southern France with a focus on Quercus pubescens. *Atmospheric Chemistry and Physics Discussions*, 14, 17225-17261.

Giorgi F. & Lionello P. (2008). Climate change projections for the Mediterranean region. *Global and Planetary Change*, 63, 90-104.

Guenther A., Hewitt C.N., Erickson D., Fall R., Geron C., Graedel T., Harley P., Klinger L., Lerdau M., McKay W.A., Pierce T., Scholes B., Steinbrecher R., Tallamraju R., Taylor J. & Zimmerman P. (1995). A global model of natural volatile organic compound emissions. *Journal of Geophysical Research: Atmospheres*, 100, 8873-8892.

Guenther A., Jiang X., Heald C., Sakulyanontvittaya T., Duhl T., Emmons L. & Wang X. (2012). The Model of Emissions of Gases and Aerosols from Nature version 2.1 (MEGAN2. 1): an extended and updated framework for modeling biogenic emissions.

Guenther A., Karl T., Harley P., Wiedinmyer C., Palmer P. & Geron C. (2006). Estimates of global terrestrial isoprene emissions using MEGAN (Model of Emissions of Gases and Aerosols from Nature). *Atmospheric Chemistry and Physics*, 6, 3181-3210.

Guenther A.B., Zimmerman P.R., Harley P.C., Monson R.K. & Fall R. (1993). Isoprene and monoterpene emission rate variability: model evaluations and sensitivity analyses. *Journal of Geophysical Research: Atmospheres (1984–2012)*, 98, 12609-12617.

Hallquist M., Wenger J., Baltensperger U., Rudich Y., Simpson D., Claeys M., Dommen J., Donahue N., George C. & Goldstein A. (2009). The formation, properties and impact of secondary organic aerosol: current and emerging issues. *Atmospheric Chemistry and Physics*, 9, 5155-5236.

Harrison S.P., Morfopoulos C., Dani K., Prentice I.C., Arneth A., Atwell B.J., Barkley M.P., Leishman M.R., Loreto F. & Medlyn B.E. (2013). Volatile isoprenoid emissions from plastid to planet. *New Phytol.*, 197, 49-57.

Hayward S., Tani A., Owen S.M. & Hewitt C.N. (2004). Online analysis of volatile organic compound emissions from Sitka spruce (Picea sitchensis). *Tree Physiology*, 24, 721-728.

Heikes B.G., Chang W., Pilson M.E., Swift E., Singh H.B., Guenther A., Jacob D.J., Field B.D., Fall R. & Riemer D. (2002). Atmospheric methanol budget and ocean implication. *Global Biogeochemical Cycles*, 16, 80-1-80-13.

Hüve K., Christ M., Kleist E., Uerlings R., Niinemets Ü., Walter A. & Wildt J. (2007). Simultaneous growth and emission measurements demonstrate an interactive control of methanol release by leaf expansion and stomata. *Journal of experimental botany*, 58, 1783-1793.

IPCC (2013). In: *Contribution of working group I to the fith assessment report of the intergovernmental panel on climate change*. Cambridge Univeristy Press Cambridge.

Jacob D.J., Field B.D., Jin E.M., Bey I., Li Q., Logan J.A., Yantosca R.M. & Singh H.B. (2002). Atmospheric budget of acetone. *Journal of Geophysical Research: Atmospheres (1984–2012)*, 107, ACH 5-1-ACH 5-17.

Jardine J. (2008). Plant physiological and environmental controls over the exchange of acetaldehyde between forest canopies and the atmosphere. *Biogeosciences*, 5.
Jimenez J., Canagaratna M., Donahue N., Prevot A., Zhang Q., Kroll J.H., DeCarlo P.F., Allan J.D., Coe H. & Ng N. (2009). Evolution of organic aerosols in the atmosphere. *Science*, 326, 1525-1529.
Keenan T., Niinemets Ü., Sabate S., Gracia C. & Peñuelas J. (2009). Process based inventory of isoprenoid emissions from European forests: model comparisons, current knowledge and uncertainties. *Atmospheric Chemistry and Physics Discussions*, 9, 6147-6206.
Kesselmeier J. & Staudt M. (1999). Biogenic volatile organic compounds (VOC): an overview on emission, physiology and ecology. *Journal of Atmospheric Chemistry*, 33, 23-88.
Lippmann M. (1989). Health effects of ozone a critical review. *Japca*, 39, 672-695.
Liu Y., Siekmann F., Renard P., El Zein A., Salque G., El Haddad I., Temime-Roussel B., Voisin D., Thissen R. & Monod A. (2012). Oligomer and SOA formation through aqueous phase photooxidation of methacrolein and methyl vinyl ketone. *Atmospheric Environment*, 49, 123-129.
Menut L., Bessagnet B., Khvorostyanov D., Beekmann M., Blond N., Colette A., Coll I., Curci G., Foret G. & Hodzic A. (2014). CHIMERE 2013: a model for regional atmospheric composition modelling. *Geoscientific Model Development*, 6, 981-1028.
Millet D.B., Guenther A., Siegel D.A., Nelson N.B., Singh H.B., de Gouw J.A., Warneke C., Williams J., Eerdekens G. & Sinha V. (2010). Global atmospheric budget of acetaldehyde: 3-D model analysis and constraints from in-situ and satellite observations. *Atmospheric Chemistry and Physics*, 10, 3405-3425.
Monson R.K., Trahan N., Rosenstiel T.N., Veres P., Moore D., Wilkinson M., Norby R.J., Volder A., Tjoelker M.G. & Briske D.D. (2007). Isoprene emission from terrestrial ecosystems in response to global change: minding the gap between models and observations. *Philosophical Transactions of the Royal Society of London A: Mathematical, Physical and Engineering Sciences*, 365, 1677-1695.
Nardini A. & Pitt F. (1999). Drought resistance of Quercus pubescens as a function of root hydraulic conductance, xylem embolism and hydraulic architecture. *New Phytol.*, 143, 485-493.
Niinemets Ü. (2010). Mild versus severe stress and BVOCs: thresholds, priming and consequences. *Trends in plant science*, 15, 145-153.
Niinemets Ü., Loreto F. & Reichstein M. (2004). Physiological and physicochemical controls on foliar volatile organic compound emissions. *Trends in plant science*, 9, 180-186.
Oikawa P.Y. & Lerdau M.T. (2013). Catabolism of volatile organic compounds influences plant survival. *Trends in plant science*, 18, 695-703.
Ormeno E., Goldstein A. & Niinemets Ü. (2011). Extracting and trapping biogenic volatile organic compounds stored in plant species. *TrAC Trends in Analytical Chemistry*, 30, 978-989.
Owen S., Harley P., Guenther A. & Hewitt C. (2002). Light dependency of VOC emissions from selected Mediterranean plant species. *Atmospheric environment*, 36, 3147-3159.
Papiez M.R., Potosnak M.J., Goliff W.S., Guenther A.B., Matsunaga S.N. & Stockwell W.R. (2009). The impacts of reactive terpene emissions from plants on air quality in Las Vegas, Nevada. *Atmospheric Environment*, 43, 4109-4123.
Polade S.D., Pierce D.W., Cayan D.R., Gershunov A. & Dettinger M.D. (2014). The key role of dry days in changing regional climate and precipitation regimes. *Scientific reports*, 4.
Pollmann J., Ortega J. & Helmig D. (2005). Analysis of atmospheric sesquiterpenes: Sampling losses and mitigation of ozone interferences. *Environmental science & technology*, 39, 9620-9629.
Quézel P. & Médail F. (2003). *Ecologie et biogéographie des forêts du bassin méditerranéen*. Elsevier Paris.
Reig-Armiñana J., Calatayud V., Cerveró J., Garcıa-Breijo F., Ibars A. & Sanz M. (2004). Effects of ozone on the foliar histology of the mastic plant (Pistacia lentiscus L.). *Environmental Pollution*, 132, 321-331.
Rinne H., Guenther A., Greenberg J. & Harley P. (2002). Isoprene and monoterpene fluxes measured above Amazonian rainforest and their dependence on light and temperature. *Atmospheric Environment*, 36, 2421-2426.
Seco R., Penuelas J. & Filella I. (2008). Formaldehyde emission and uptake by Mediterranean trees *Quercus ilex* and *Pinus halepensis*. *Atmospheric Environment*, 42, 7907-7914.
Sharkey T.D. & Yeh S. (2001). Isoprene emission from plants. *Annual review of plant biology*, 52, 407-436.
Singh H., Chen Y., Tabazadeh A., Fukui Y., Bey I., Yantosca R., Jacob D., Arnold F., Wohlfrom K. & Atlas E. (2000). Distribution and fate of selected oxygenated organic species in the troposphere and lower stratosphere over the Atlantic. *Journal of Geophysical Research: Atmospheres (1984–2012)*, 105, 3795-3805.
Smiatek G. & Steinbrecher R. (2006). Temporal and spatial variation of forest VOC emissions in Germany in the decade 1994–2003. *Atmospheric Environment*, 40, 166-177.
Velikova V., Várkonyi Z., Szabó M., Maslenkova L., Nogues I., Kovács L., Peeva V., Busheva M., Garab G. & Sharkey T.D. (2011). Increased thermostability of thylakoid membranes in isoprene-emitting leaves probed with three biophysical techniques. *Plant Physiology*, 157, 905-916.

Vlasenko A., Macdonald A., Sjostedt S. & Abbatt J. (2010). Formaldehyde measurements by Proton transfer reaction–Mass Spectrometry (PTR-MS): correction for humidity effects. *Atmospheric Measurement Techniques*, 3, 1055-1062.

Von Caemmerer S.v. & Farquhar G. (1981). Some relationships between the biochemistry of photosynthesis and the gas exchange of leaves. *Planta*, 153, 376-387.

Xie X., Shao M., Liu Y., Lu S., Chang C.-C. & Chen Z.-M. (2008). Estimate of initial isoprene contribution to ozone formation potential in Beijing, China. *Atmospheric Environment*, 42, 6000-6010.

Table:

Table 1: Net photosynthesis (*Pn*, µmolCO_2 m^{-2} s^{-1}), stomatal conductance to water (*Gw*, mmolH_2O m^{-2} s^{-1}) and emission rates (µgC g_{DM}^{-1} h^{-1}) according to treatment and season. Values represent an average of all data measured between 12h and 15h (local time). Letters denote the difference between drought treatments with a > b ($P < 0.05$) and values showed represent the mean ± SE, n=5. ND: natural drought and AD: amplified drought.

Season	**Spring**		**Summer**		**Autumn**	
Treatment	**ND**	**AD**	**ND**	**AD**	**ND**	**AD**
Pn	10.6 ± 0.7a	9.1 ± 1.7a	13.6 ± 2.3a	8.7 ±1.2b	7.2 ±0.8a	9.1 ± 1.0a
Gw	107.7± 18.6a	56.6± 13.1b	285.4± 37.7a	125.9± 17.4b	122.5± 23.4a	74.1 ± 21.1a
Isoprene	20.3 ± 3.8a	10.2 ± 2.3b	124.3± 10.2a	81.1 ± 11.0b	3.0 ± 0.6a	5.2 ± 1.5a
MACR+MVK +ISOPOOH	0.12 ± 0.03a	0.06 ± 0.01a	0.4 ± 0.05a	0.2 ± 0.02b	0.04 ± 0.01a	0.06 ± 0.01a
Methanol	0.8 ± 0.1a	0.5 ±0.04b	1.0 ± 0.2a	0.6 ± 0.03b	0.2 ± 0.03a	0.2 ± 0.05a
Acetaldehyde	1.4 ± 0.4a	0.9 ± 0.3a	2.0 ± 0.5a	1.1 ± 0.1a	1.2 ± 0.3a	1.2 ± 0.3a
Acetone	0.5 ± 0.1a	0.2 ± 0.02a	1.1 ± 0.2a	0.5 ± 0.04b	0.4 ± 0.1a	0.4 ± 0.1a
Formaldehyde	0.2 ± 0.05a	0.1± 0.01a	0.4 ± 0.07a	0.1 ± 0.02b	0.2 ± 0.05a	0.3 ± 0.06a

Figure legends

Figure 1: Ombrothermic diagram for natural and amplified drought in 2012, 2013 and 2014. Bars represent mean monthly precipitation (mm) and curves represent mean monthly temperature (°C). On each amplified drought graph, the percentage represents the proportion of excluded rain compared to natural drought plot.

Figure 2: Diurnal pattern of stomatal conductance (*Gw*) and net photosynthesis (*Pn*) according to drought treatment and season**.** Values showed represent means ± SE, n=5.

Figure 3: Diurnal pattern of isoprene emissions rates, where points represent measured emissions, and the yellow line correspond to modelled emissions rates according to the *L+T* algorithm (ER_{L+T}) Values are mean ± SE, n=5. R^2 and slope (sl) of correlations between measured and modelled emissions are presented in the yellow frame. Correlations were obtained without forcing data through the origin.

Figure 4: Diurnal pattern of acetaldehyde emissions rates, where points represent measured emissions, the yellow line correspond to modelled emissions rates according to the *L+T* algorithm (ER_{L+T}) and dotted line is modelled emissions rates according to *T* algorithm (ER_T). Values are mean ± SE, n=5. R^2 and slope (sl) of correlations between measured and modelled emissions are presented in the yellow frame for *L+T* and in the white frame for *T*. Correlations were obtained without forcing data through the origin.

Figure 5: Diurnal pattern of measured methanol emissions rates. Points (means ± SE, n=5) represent measured emissions, yellow line correspond to modelled emissions rates according to the *L+T* algorithm (ER_{L+T}) and dotted line is modelled emissions rates according to *T* algorithm (ER_T). Values are mean ± SE, n=5. R^2 and slope (sl) of correlations between measured and modelled emissions are presented in the yellow frame for *L+T* and in the white frame for *T*. Correlations were obtained without forcing data through the origin.

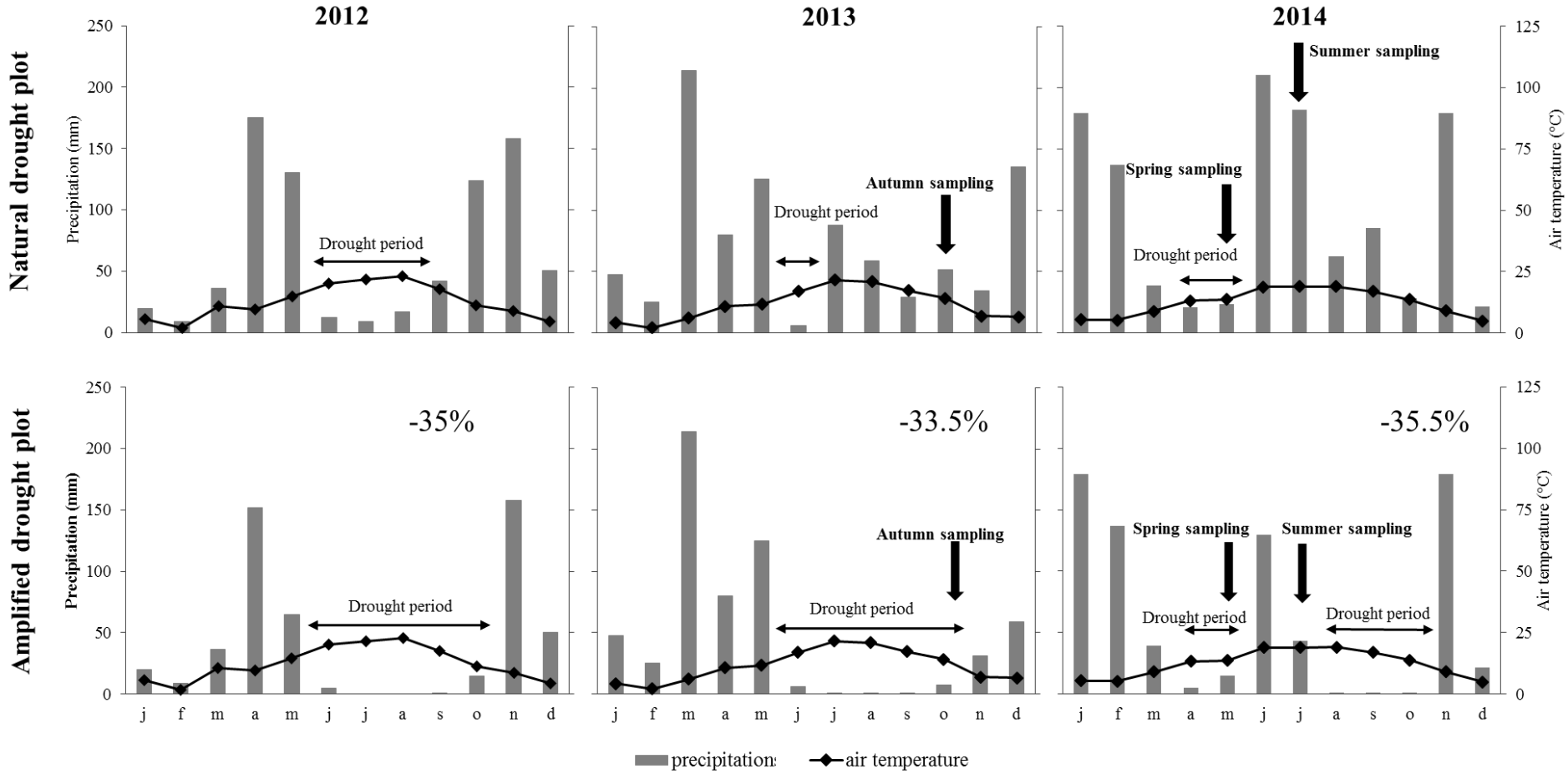

572

573 **Figure 1:**

574

575

576

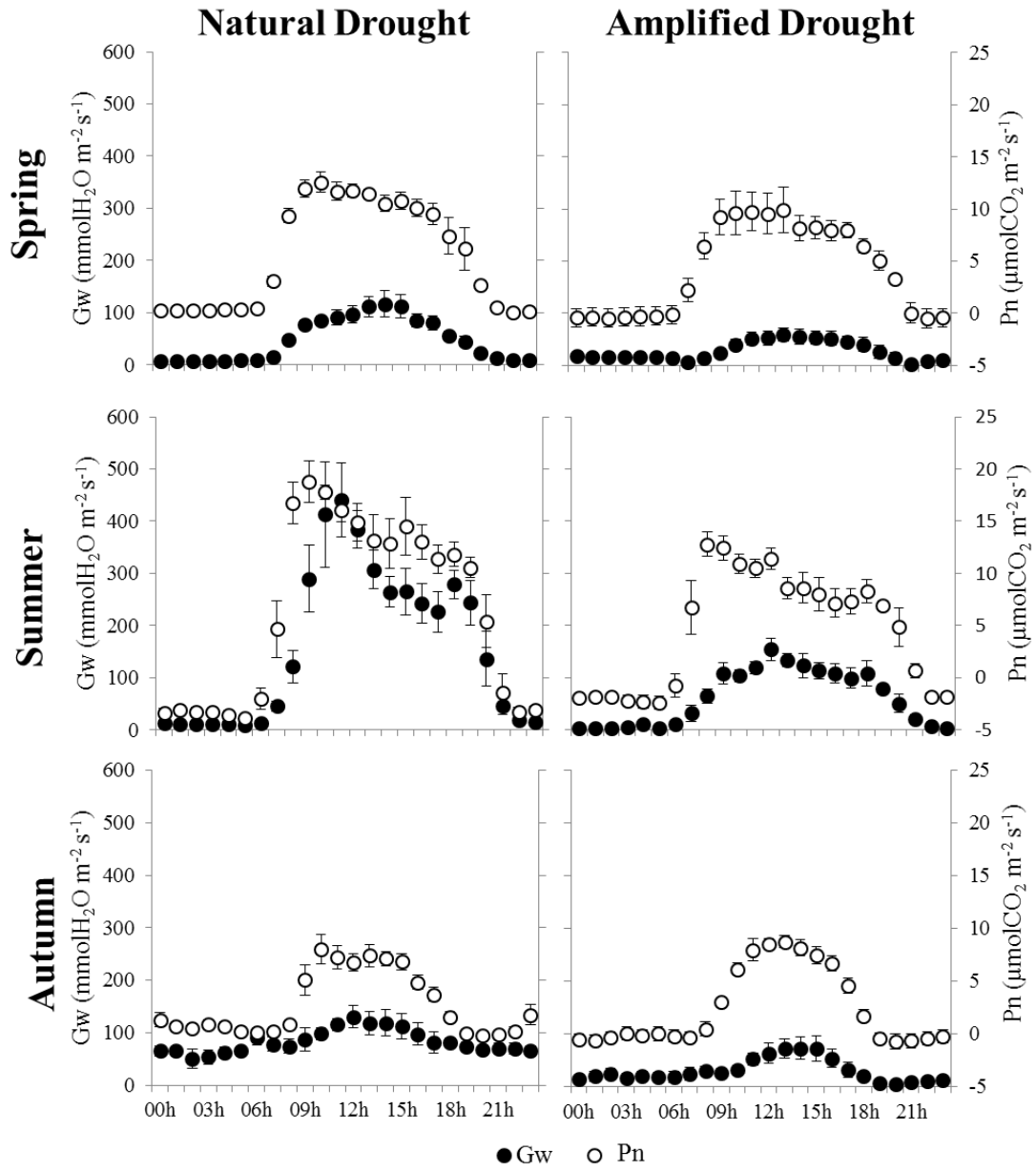

577

578 **Figure 2:**

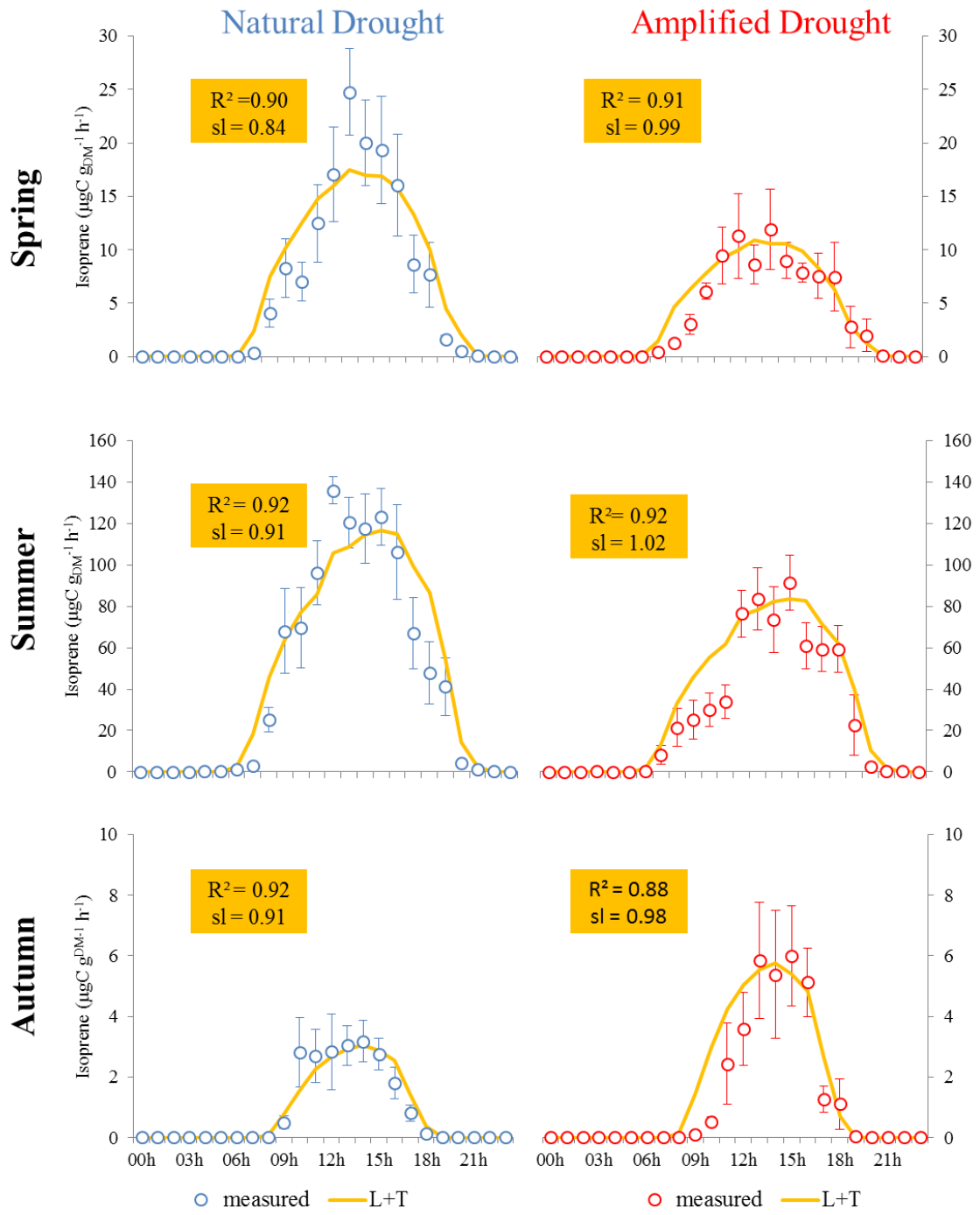

579

580 **Figure 3:**

581

582

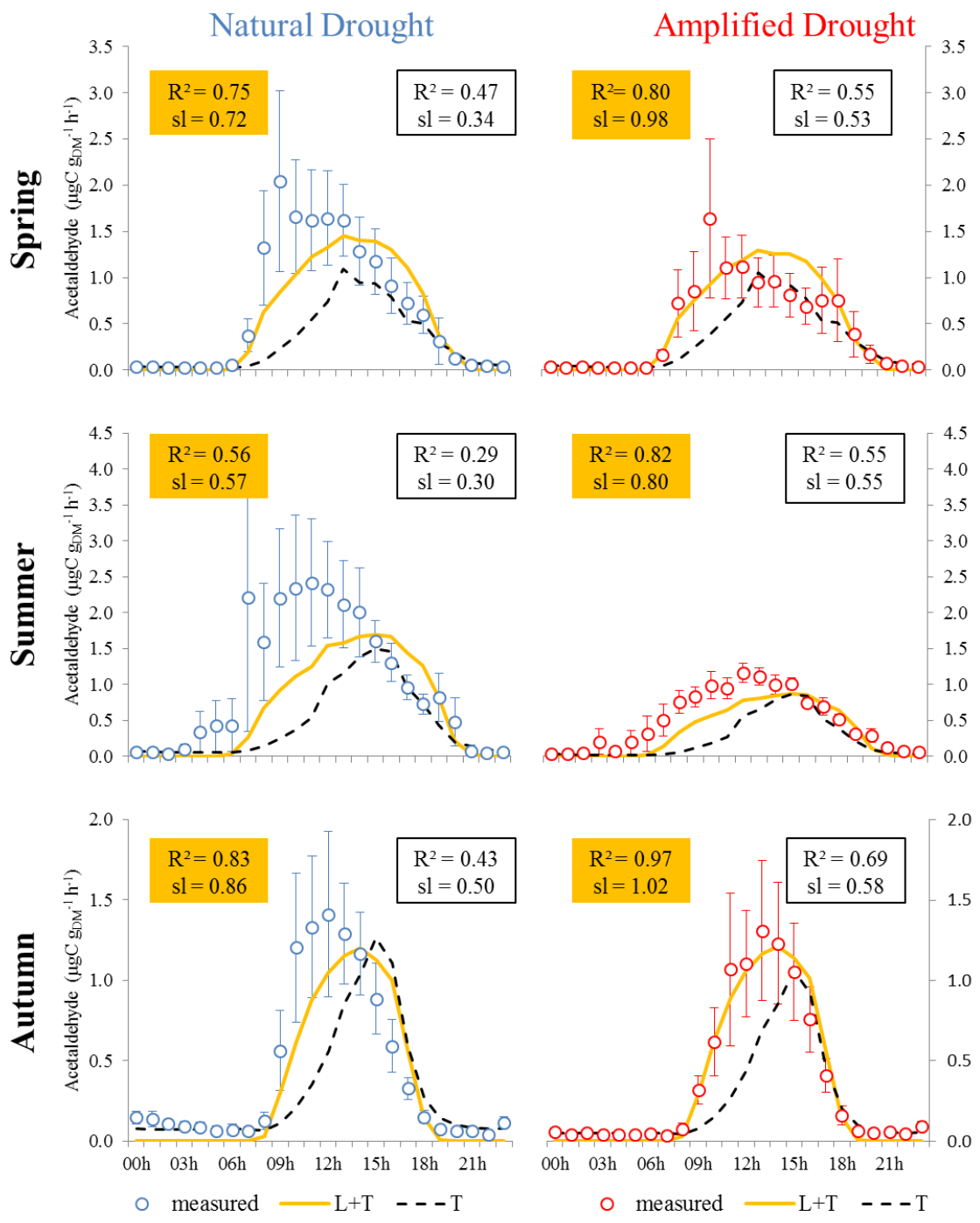

583

584 **Figure 4:**

585

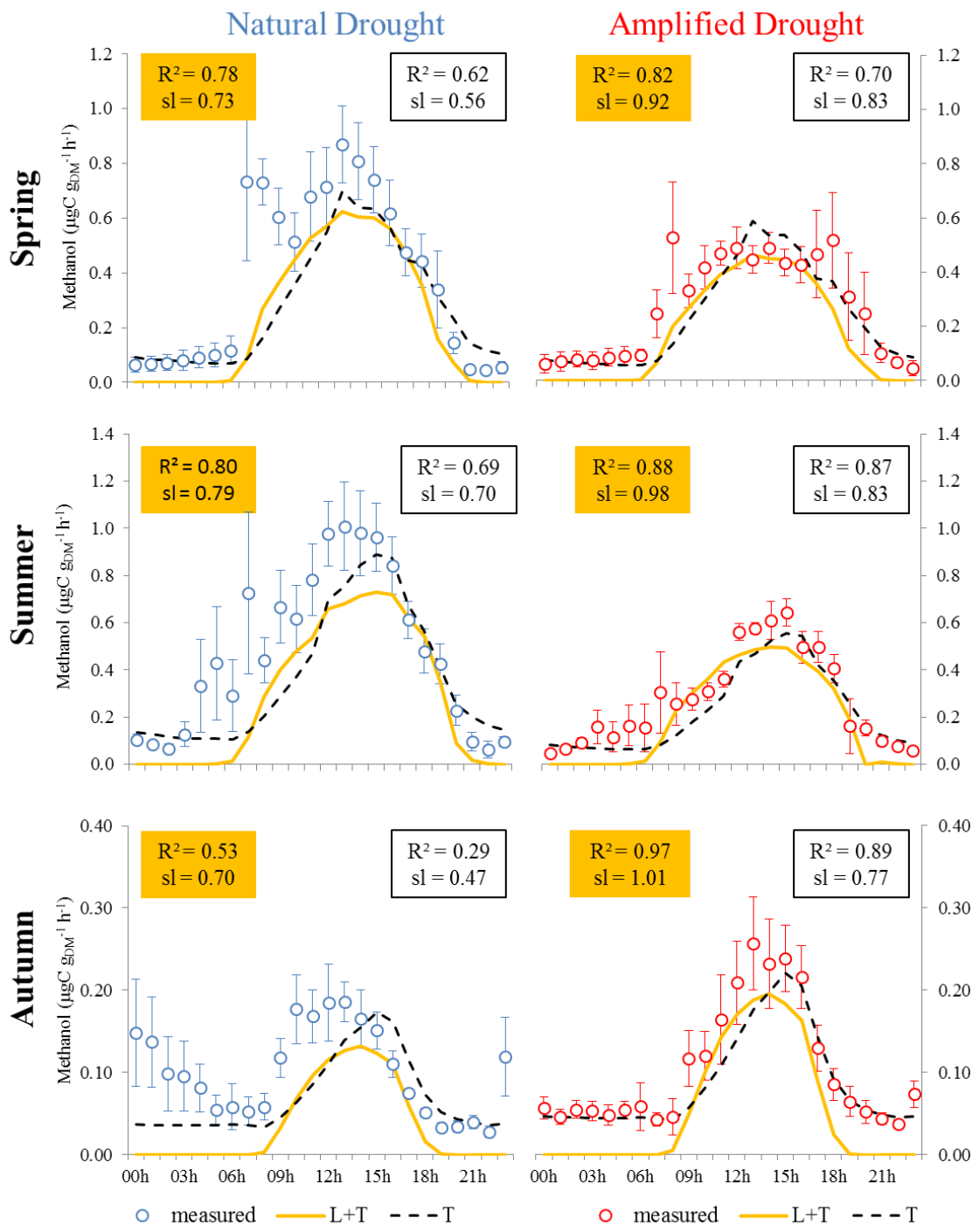
Natural Drought
Amplified Drought
Spring
Summer
Autumn
Methanol (µgC g$_{DM}^{-1}$ h^{-1})
R² = 0.78
sl = 0.73
R² = 0.62
sl = 0.56
R² = 0.82
sl = 0.92
R² = 0.70
sl = 0.83
R² = 0.80
sl = 0.79
R² = 0.69
sl = 0.70
R² = 0.88
sl = 0.98
R² = 0.87
sl = 0.83
R² = 0.53
sl = 0.70
R² = 0.29
sl = 0.47
R² = 0.97
sl = 1.01
R² = 0.89
sl = 0.77
00h 03h 06h 09h 12h 15h 18h 21h
measured
L+T
T

Figure 5: